BBA - Molecular Cell Research 1871 (2024) 119651

Contents lists available at ScienceDirect

BBA - Molecular Cell Research

journal homepage: www.elsevier.com/locate/bbamcr

Research paper

Peripheral 5-HT/HTR6 axis is responsible for obesity-associated hypertension

Vadim I. Chechekhin [a,1], Anastasia M. Ivanova [a,1], Konstantin Y. Kulebyakin [a], Yulia G. Antropova [a], Maxim N. Karagyaur [a], Maria N. Skryabina [a], Elizaveta S. Chechekhina [a], Natalia A. Basalova [a,b], Olga A. Grigorieva [a,b], Veronika Yu Sysoeva [a], Natalia I. Kalinina [a], Vsevolod A. Tkachuk [a,b], Pyotr A. Tyurin-Kuzmin [a,*]

[a] Department of Biochemistry and Molecular Medicine, Faculty of Medicine, Lomonosov Moscow State University, Moscow 119991, Russia
[b] Institute for Regenerative Medicine, Medical Research and Educational Center, Lomonosov Moscow State University, Moscow 119991, Russia

ARTICLE INFO

Keywords:
Peripheral 5-HT
Serotonin
Mesenchymal stromal cells
Mural cells
Adipose tissue
HTR6

ABSTRACT

Hypertension is one of the major life-threatening complications of obesity. Recently adipose multipotent mesenchymal stromal cells (MSCs) were implicated to the pathogenesis of obesity-associated hypertension. These cells amplify noradrenaline-induced vascular cell contraction via cAMP-mediated signaling pathway. In this study we tested the ability of several cAMP-mediated hormones to affect the adrenergic sensitivity of MSCs and their associated contractility. Despite that adipose MSCs express a plethora of receptors capable of cAMP signaling activation, only 5-HT was able to elevate α1A-adrenoceptor-induced Ca^{2+} signaling in MSCs. Furthermore, 5-HT markedly enhanced noradrenaline-induced MSCs contractility. Using HTR isoform-specific antagonists followed by CRISPRi-mediated knockdown, we identified that the observed 5-HT effect on MSCs was mediated by the HTR6 isoform. This receptor was previously associated exclusively with 5-HT central nervous system activity. Discovered effect of HTR6 on MSCs contractility points to it as a potential therapeutic target for the prevention and treatment of obesity-associated hypertension.

1. Introduction

Adipose tissue growth and remodeling ultimately involve a heterogeneous multiplicity of stromal cells, including multipotent mesenchymal stromal cells (MSC) [1,2]. Although it is well established that MSCs control the growth of adipose tissue, their function is much wider than merely differentiation into new adipocytes. At least a part of MSCs exhibit pericyte distribution and functions: they are situated in association with the endothelium of small vessels and express pericyte markers including PDGFRb and NG2 [3]. Recently it was established that these cells control noradrenaline-induced vascular contraction and thus could contribute to the development of obesity-associated hypertension [4].

In adipose tissue, vascular cell contraction is mediated by the activation of intracellular Ca^{2+} mobilization triggered by α1A-adrenoceptors. Interestingly, α1A-adrenoceptors are exclusively present on the surface of perivascular PDGFRb-positive MSCs, but not on smooth muscle cells [4]. This α1A-adrenoceptor signaling plays a crucial role in the event of obesity. Sympathetic outflow increases during obesity, resulting in a subsequent activation of not only α1A-adrenoceptor/Ca^{2+} but also β3-adrenoceptors/cAMP intracellular cascades. Such cAMP-signaling is responsible for a noticeable amplification of α1A-adrenoceptor-induced Ca^{2+} signaling in MSC/pericytes of small vessels resulting in the formation of contractile cell phenotype [5,6]. These findings point to cAMP-cascade activation in adipose MSC as an upstream factor responsible for obesity-associated hypertension.

Noradrenaline is not the only hormone that induces cAMP signaling in MSCs. Their functions are regulated by a number of cAMP-mediated hormones, such as 5-HT, histamine, adenosine and dopamine. These hormones activate functional responses in MSCs/pericytes [7], including immunoregulatory function and differentiation [8,9]. In our study, we analyzed the ability of these cAMP-mediated hormones to affect the adrenergic sensitivity of MSCs and their associated contractile properties. Surprisingly, we observed that among other cAMP-activating hormones only 5-HT was able to elevate α1A-adrenoceptor-induced

* Corresponding author.
E-mail address: tyurinkuzmin.p@gmail.com (P.A. Tyurin-Kuzmin).
[1] These two authors contributed equally to this work

https://doi.org/10.1016/j.bbamcr.2023.119651
Received 10 July 2023; Received in revised form 5 December 2023; Accepted 5 December 2023
Available online 11 December 2023

Ca^{2+} signaling in MSCs and markedly enhance their contractility. Discovered effect of this 5-HT receptor on MSCs contractility points to it as a potential therapeutic target for the prevention and treatment of obesity-associated hypertension.

2. Materials and methods

2.1. MSC isolation and culturing

MSCs were isolated from subcutaneous fat tissue of 34 young donors (age 42.89 ± 1.98 years; BMI 29.46 ± 0.90 kg/m^2, for detailed information see Supplemental Table 1) using enzymatic digestion as previously described [10,11]. The work was carried out in accordance with The Code of Ethics of the World Medical Association (Declaration of Helsinki). All donors gave their informed consent and the local ethics committees of Burdenko Main Military Clinical Hospital (Moscow, Russia) and the Medical Research and Education Center of Lomonosov Moscow State University (IRB00010587, Moscow, Russia) approved the study protocol (#4, 4 June 2018). ASC52telo, hTERT immortalized adipose derived mesenchymal stem cells (ATCC®SCRC-4000™) were obtained from ATCC (Manassas, VA, USA). Primary and hTERT immortalized MSCs were cultured in AdvanceSTEM Mesenchymal Stem Cell Media containing 10 % AdvanceSTEM Supplement (HyClone, Cytiva, USA), 1 % antibiotic–antimycotic solution (HyClone, Cytiva, USA) at 37 °C in a 5 % CO_2 incubator (Binder, Tuttlingen, Germany, CB210). Cells were passaged at 70–80 % confluency using Versen solution (Paneco, Russia) and HyQTase solution (HyClone, Cytiva, USA). For the experiments, MSCs cultured up to 4th–5th passages were used. To confirm their multipotency, MSCs were induced into osteogenic, adipogenic, and chondrogenic differentiation as described earlier [12].

2.2. Collagen gel contraction assay

Collagen gel contraction assay was performed as described previously [13]. Briefly, cells were trypsinized and centrifuged. 100.000 cells per well in DMEM were added to the collagen (P C11-NCL, Imtek) neutralized with 1 M NaOH (3 mg/ml in 0.1 % acetic acid, Imtek). The matrix was allowed to polymerize at RT for 30 min. Then Advance stem medium with 10 % supplement was added and the matrix disk was detached from the well walls to allow contraction. Noradrenaline or 5-HT were added to the culture medium 30 min after detaching; 1 h later disks were washed off with DMEM LG and medium was changed on fresh Advance stem with 10 % supplement. Noradrenaline has been added again to the culture medium 6 h after adding the first stimulus. Matrix disk area was measured before the second stimuli and 2, 12, 24 28 h after using Nikon SMZ18. % matrix contraction was calculated as: (area of the shortened disk) / (area of disk before stimulus) * 100.

2.3. MSC treatment and Ca^{2+} imaging

Adrenergic receptor and serotonergic receptor activation were assessed using either noradrenaline (Abcam, ab120717, 1 μM, Cambridge, UK) or 5-HT (Abcam, ab120528, 10 μM, Cambridge, UK) and Ca^{2+} imaging. Briefly, cells grown in HyClone Advance Stem medium with Supplement in 48 well plates were loaded with Fluo-8 (Abcam, ab142773, 4 μM), in Hanks Balanced Salt Solution with 20 mM Hepes, for 1 h. Cells were grown at low density to prevent cell-to-cell communications during the calcium imaging. To analyze the amount of functionally active cells after pretreatment with noradrenaline or 5-HT we stimulated cells with hormones for 1 h, washed them three times using Hanks Balanced Salt Solution (PanEco, Russia), and incubated the cells in full growth medium for an additional 5 h. To evaluate what isoforms of serotonergic receptors regulated the number of MSC responding to noradrenaline we treated cells with either HTR6-antagonist R1485 (Tocris, Cat# 4964, 1 μM) or HTR7-antagonist SB258719 (Tocris, Cat# 2726, 10 μM) 30 min before Ca^{2+} imaging. Cells were loaded with Fluo-8 for 1 h before the experiment. To measure the percent of responded cells we recorded the baseline for 5 min then once added noradrenaline. Ca^{2+} transients were measured in individual cells using an inverted fluorescent microscope Nikon Eclipse Ti equipped with an objective CFI Plan Fluor DLL 10×/0.3 (Nikon, Tokyo, Japan) and with digital EMCCD camera Andor iXon 897 (Andor Technology, Belfast, UK) and Nikon Eclipse Ti2 equipped with an objective CFI Plan Fluor DL 10XF CH, NA0.3 (Nikon, Tokyo, Japan) and with digital sCMOS camera Photometrics Kinetix. We used the simultaneous measuring of 6 × 6 fields of view in Large Image mode to increase the number of analyzed cells. Movies were analyzed using NIS-Elements (Nikon, Tokyo, Japan) and ImageJ software. Alterations of cytosolic Ca^{2+} from the resting level were quantified by relative changes in the intensity of Fluo-8 fluorescence (ΔF/F0) recorded from an individual cell. The percent of responded cells was measured as the ratio of the number of responded cells to the number of all analyzed cells in 6 × 6 fields of view.

2.4. PCR

Total RNA was isolated and purified using the RNeasy mini kit (Qiagen, Germantown, MD, USA) according to the manufacturer's instructions. The RNA was quantified using Nanodrop 1000 spectrophotometer (Thermo Fisher Scientific, Wellington, USA). For cDNA preparation, 1 μg of total RNA was used. Reverse transcription was performed using an MMLV RT kit (Cat#SK022L, Evrogen), oligo-dT primers (Cat#SB001, Evrogen) and dNTP (Cat#PB006S, Evrogen). cDNA was synthesized as described in the manufacturer's protocol. Real-time PCR was performed using qPCRmix-HS SYBR+LowROX kit (Cat#PK156L, Evrogen) and CFX96 Touch Real-Time PCR Detection System (BioRad, USA) with the following protocol:

1. Initial denaturation at 95 °C for 3 min,
2. 40 cycles of:
1. Denaturation at 95 °C for 10 s,
2. Annealing at 64 °C for 10 s (empirically matched primer-specific temperature),
3. Elongation at 72 °C for 30 s with plate reading,
4. Denaturation at 95 °C for 10 s,
5. Melting curves were obtained with temperatures ranging from 65 °C to 95 °C with a 0,5 °C increase every 5 s with plate reading.

Treated cells were compared with control samples without hormones addition. The quantitative analysis was achieved by the ΔΔCt method using PRL13A as a reference gene. Primers sequences are listed in the Key Resource Table.

2.5. Western-blotting

Cells were grown to 60 % confluence in 100 mm Petri dishes with DMEM LG (Gibco, USA) containing 10 % FBS (Gibco, USA) and 1 % antibiotic–antimycotic solution (HyClone, USA). In the case of the experiment with preincubation the cells were stimulated with 10^{-5} M 5-HT or vehicle, incubated for 1 h, and washed three times with a growth medium. 6 h after stimulation cell medium was quickly removed and the dishes were transferred on ice. The cells were rinsed with ice-cold phosphate-buffered saline (5.2 mM Na2HPO4, pH 7.4 and 150 mM NaCl) and scraped by rubber cell scraper (Corning) in 3× SDS sample buffer without β-mercaptoethanol (6 % SDS, 0.2 M Tris, pH 6.8, 40 % glycerol and 0.03 % bromophenol blue). Samples were passed 5 times through a 30-gauge needle to splinter DNA. Total protein concentration was measured using Bio-Rad protein assay based on the Bradford dye-binding method (BioRad, USA). Then 50 μl of β-mercaptoethanol was added per 1 ml of sample. After β-mercaptoethanol addition samples were boiled for 5 min and cooled on ice.

Proteins were separated by Any kD Mini-PROTEAN TGX Stain-Free Protein Gels (BioRad, USA) in the Mini-PROTEAN 3 BioRad Units

using Tris/Glycine/SDS buffer (diluted from 10× premixed electrophoresis buffer, containing 25 mM Tris, 192 mM glycine, 0.1 % SDS, pH 8.3, BioRad, USA). The loading amount was controlled by immunostaining for vinculin. The proteins were transferred onto 0.45 μm polyvinylidene fluoride (PVDF) membranes (Amersham, USA) for 1 h at 350 mA in the buffer containing 25 mM Tris, 0.192 M glycine, pH 8.3, 20 % ethanol, 0.02 % sodium lauryl sulfate. The membranes were blocked for 1 h in 5 % non-fat milk in TBST (25 mM Tris/HCl, pH 7.4, 150 mM NaCl, 0.1 % Tween-20). The membranes were incubated overnight at 4 °C with primary antibody to α1A-adrenoceptors (ab137123, Abcam, Cambrige) and to HTR6 (Affinity Bioscience DF3505), UK in a dilution recommended by the supplier, washed 3 times in TBST, and incubated for 1 h at room temperature with the peroxidase-conjugated secondary antibodies. All blocking procedures, antibody incubation, and washings were carried out in TBST (25 mM Tris/HCl, pH 7.4, 150 mM NaCl, 0.1 % Tween-20) supplemented with 5 % dry nonfat milk. The protein bands were visualized by enhanced chemiluminescence (ECL, West Pico, Pierce, USA) on the ChemiDoc Imaging System (BioRad, USA). Each membrane was developed for at least two different time intervals to ensure the linearity of the ECL signal. The quantitative analysis was achieved using ChemiDoc Imaging System (BioRad, USA) software.

2.6. Immunofluorescent detection of HTR6

Subcutaneous fat tissue was obtained during abdominal surgery. Part of each sample was placed in O.C.T. Compound (Sakura Inc., Tokyo, Japan) and frozen in liquid nitrogen for immunofluorescent analysis. HTR6 was visualized by immunofluorescent staining of 12 μm frozen sections using antibodies against HTR6 (Affinity Bioscience, DF3505). Specificity of antibodies was tested by immunostaining of mouse brain frozen sections (coronal region). We found strong specific (comparing to control IgG) immunostaining in the dentate gyrus molecular layer (DG), pyramidal layer of hippocampus formation (C1), and paraventricular nucleus of thalamus (PVT), which are characteristic regions of HTR6 expression in the brain (Supplementary Fig. 1). Sections of adipose tissue were fixed in 4 % paraformaldehyde for 10 min. After several washes by phosphate buffer saline (PBS) sections were incubated in 1 % bovine serum albumine (BSA) containing 10 % normal donkey serum to block non-specific binding of antibodies. This was followed by incubation with specific primary antibodies, for 1 h and subsequent extensive washing in PBS. Then sections were incubated with Alexa488-conjugated donkey anti-rabbit (Thermo Fisher Scientific). To assess the co-localization of cells expressing HTR6, β3-adrenergic receptors and blood vessels, we performed double immunofluorescent staining: sections were incubated with mix of antibodies HTR6, β3-adrenergic receptors (Abnova, H00000155-B01P) and antibodies to endothelial cells (CD31, Abcam, ab24590) or smooth muscle cells (alpha-SMA, M0851, Dako) or pericytes/mesenchymal stem cells (PDGFRb, P7679, Sigma-Aldrich). This was followed by incubation with Alexa488-conjugated donkey anti-rabbit antibody (Thermo Fisher Scientific) and Alexa594-conjugated goat anti-mouse antibody (Thermo Fisher Scientific). Cell nuclei were counterstained with DAPI (D9542, Sigma-Aldrich), and sections were mounted in Aqua Poly/Mount (Cat#18606, Polysciences Inc). For negative controls mouse or rabbit non-specific IgGs were used in appropriate concentration. Images were obtained using confocal microscope LSM 780 and ZEN2010 software (Zeiss).

2.7. Flow cytometry analysis

Co-expression of HTR6 and β3-adrenergic receptors were analyzed using flow cytometry. After medium harvesting cells were detached from culture dishes using HyQTase solution (HyClone, Cytiva, USA), and stained with antibodies against HTR6 (Affinity Bioscience, DF3505) and β3 (Abnova, H00000155-B01P), following by secondary antibodies Alexa488-conjugated donkey anti-mouse antibody (Thermo Fisher Scientific) and Alexa594-conjugated goat anti-rabbit antibody (Thermo Fisher Scientific) on formalin fixed non permeabilized cells. Normal rabbit IgG (10500C, Invitrogen, 1:300) and normal mouse IgG1 (Dako X0931, 1:20) were used as a negative control. Stained cells were analyzed using FACS ARIA III cell sorter (BD, Franklin Lakes, NJ, USA). 20,000–50,000 events were acquired and analyzed for antigen expression. Fluorescence intensity was compared between means of fluorescence intensities in control and treated cells.

2.8. Down-regulation of HTR6 by CRISPR-interference

To suppress the activity of the HTR6 gene in the ASC52telo cell line, we used a modification of the CRISPRi genome editing system [14]. For this purpose, we used a modified LentiCRISPRv2GFP vector (Addgene, #82416) encoding dCas9, which does not introduce double-strand breaks in DNA but prevents the expression of the target gene (sterically blocks transcript elongation). To target the CRISPRi system to the HTR6 gene, the following gRNAs 5'-CAACCTCTGCCTCATCAGCC and 5'-GCCATGCTGAACGCGCTGTA were used, which were selected according to the previously published protocol [15] and cloned into the same LentiCRISPRv2GFP vector (Addgene, #82416) using *Bsm*BI restrction sites. Assembly of lentiviral particles encoding components of the CRISPR/Cas9 system was performed by transfection of the HEK293T cell line with the obtained LentiCRISPRv2GFP vector using linear PEI 25 kDa (Polysciences, #23966-1), as described previously [16]. Lentiviral particles encoding dCas9 and gRNA were collected, filtered through the 0.45 um syringe filter (Merck, MF-Millipore, #HAWP04700), and used for transduction of the human mesenchymal stromal cell line ASC52telo, as described previously [7]. The selection of the transduced ASC52telo cells was carried out via sorting the most GFP-bright cells using BD FACS Aria III cell sorter (BD, USA, Franklin Lakes). In the resulting ASC52telo cell population, the level of HTR6 expression and the degree of its suppression were assessed using Western Blotting.

2.9. Data representation and statistical analysis

Statistical analysis was performed using SigmaPlot 12.5 software (Systat Software Inc., San Jose, CA, USA). Data were assessed for normality of distribution using the Shapiro-Wilk test. Values are expressed as mean ± standard error of the mean (SEM). Comparison of two independent groups was performed by Student *t*-test for normally distributed data and Mann–Whitney U-criteria (M-*U* test) for not normally distributed data. Multiple comparisons were made using the Kruskal-Wallis test (one-way ANOVA on ranks) with subsequent application of Dunn criteria. Statistical significance was defined as p-value <0.05.

2.10. Key resources table

Reagent or resource	Source	Identifier
Antibodies		
Mouse monoclonal anti-Vinculin	Sigma-Aldrich	Cat#v9131; RRID: AB_477629
Rabbit monoclonal anti-alpha 1A-adrenergic receptor	Abcam	Cat#ab137123
Goat polyclonal anti-rabbit	Imtek	Cat#P-GAR Iss
Rabbit polyclonal anti-mouse	Imtek	Cat#P-RAM Iss
Rabbit polyclonal anti-Tyrosine Hydroxylase	Sigma-Aldrich	Cat#AB152; RRID: AB_390204
Mouse monoclonal anti-alpha-Smooth muscle actin	Dako	Cat#M0851; RRID: AB_2223500
Mouse monoclonal anti-PDGF Rβ	Sigma-Aldrich	Cat#P7679; RRID: AB_477399
Mouse monoclonal anti-CD31	Dako	Cat#IR610
Rabbit polyclonal anti-HTR6	Biorbyt	orb672836

(*continued on next page*)

(*continued*)

Reagent or resource	Source	Identifier
Donkey polyclonal anti-Rabbit IgG (H + L) Cross-Adsorbed Secondary Antibody, Alexa Fluor 594	Thermo Fisher Scientific	Cat#A-21207; RRID: AB_141637
Goat polyclonal anti-Mouse IgG (H + L) Cross-Adsorbed Secondary Antibody, Alexa Fluor 488	Thermo Fisher Scientific	Cat#A-11001; RRID: AB_2534069
Biological samples		
Human subcutaneous adipose tissue from bariatric procedures from multiple donors	This paper	N/A
MSCs from subcutaneous adipose tissue from multiple donors	This paper	N/A
Chemicals, peptides, and recombinant proteins		
Fluo-8 green fluorescent calcium binding dye	Abcam	ab142773
DAPI blue fluorescent nucleic acid stain	Sigma-Aldrich	Cat#D9542
R1485 5HTR$_6$-antagonist	Tocris	Cat#4964
SB258719 5HTR$_7$-antagonist	Tocris	Cat#2726
EMD-386088	Abcam	ab120328
Collagen 1	Imtek	Cat#P C11-NCL
Noradrenaline	Abcam	ab120717
Serotonin	Abcam	ab120528
Adenosine	Sigma-Aldrich	A9251
Histamine	Sigma-Aldrich	H7125
Dopamine	Sigma-Aldrich	H8502
dNTP	Evrogen	Cat#PB006S
oligo-dT primers	Evrogen	Cat#SB001
Oligonucleotides		
Primer PRL13A Forward: CTCAAGGTCGTGCGTCTGAA	This paper	N/A
Primer PRL13A Reverse: ACGTTCTTCTCGGCCTGTTT	This paper	N/A
Primer ADRA1A Forward: TGCCAGATCAACGAGGAGC	This paper	N/A
Primer ADRA1A Reverse: GGCGTTTTTCCGATGGATGC	This paper	N/A
Primer HRH2 Forward: CGTGTCCTTGGCTATCACTGA	Tyurin-Kuzmin et al., 2020	N/A
Primer HRH2 Reverse: GGCTGGTGTAGATATTGCAGAAG	Tyurin-Kuzmin et al., 2020	N/A
Primer ADORA2A Forward: CGCTCCGGTACAATGGCTT	Tyurin-Kuzmin et al., 2020	N/A
Primer ADORA2A Reverse: TTGTTCCAACCTAGCATGGGA	Tyurin-Kuzmin et al., 2020	N/A
Primer ADORA2B Forward: CTGTCACATGCCAATTCAGTTG	Tyurin-Kuzmin et al., 2020	N/A
Primer ADORA2B Reverse: GCCTGACCATTCCCACTCTTG	Tyurin-Kuzmin et al., 2020	N/A
Primer DRD1 Forward: AGGGACTTCTCTGTTCGTATCC	Tyurin-Kuzmin et al., 2020	N/A
Primer DRD1 Reverse: AGGGACTTCTCTGTTCGTATCC	Tyurin-Kuzmin et al., 2020	N/A
Primer DRD5 Forward: CCGTGTCAGACCTTTTCGTG	Tyurin-Kuzmin et al., 2020	N/A
Primer DRD5 Reverse: TGCGCTGAGTCATCTTGCG	Tyurin-Kuzmin et al., 2020	N/A
Primer HTR4 Forward: CTCACGTTTCTCTCGACGGTT	Tyurin-Kuzmin et al., 2020	N/A
Primer HTR4 Reverse: AGCAGATCCGCAAAAGCAAGA	Tyurin-Kuzmin et al., 2020	N/A
Primer HTR6 Forward: GCAACACGTCCAACTTCTTCC	Tyurin-Kuzmin et al., 2020	N/A
Primer HTR6 Reverse: TGCAGCACATCACGTCGAA	Tyurin-Kuzmin et al., 2020	N/A
Primer HTR7 Forward: CGAAGATGATTCTCTCCGTCTG	Tyurin-Kuzmin et al., 2020	N/A
Primer HTR7 Reverse: GCGGTAGAGTAAATCGTATAGCC	Tyurin-Kuzmin et al., 2020	N/A
Software and algorithms		
ZEN2010	Zeiss	https://www.zeiss.com/microscopy/int/products/microscope-software/zen-lite.html
NIS-Elements 5.21.02	Nikon BioImaging Lab	https://www.microscope.healthcare.nikon.com/
ImageJ 1.52i	Schneider et al., 2012	https://imagej.nih.gov/ij/
SigmaPlot 12.5	SigmaPlot	http://www.sigmaplot.co.uk/index.php

(*continued on next column*)

3. Results

3.1. 5-HT enhances α1A-adrenoceptor dependent MSCs contractility

Earlier we have demonstrated that noradrenaline increases the MSCs' responsiveness to itself. Despite noradrenaline causes a rapid desensitization of β -adrenoceptors on MSCs, it also induces a significant increase in quantity and sensitivity of α1A -adrenoceptor 6 h later. Such increase was due to the activation of β3-adrenoceptors and cAMP intracellular cascades. [4,6]. To elucidate which other hormones could affect alpha1A-adrenoceptor sensitivity on MSCs, we analyzed an expression profile of receptors coupled to cAMP pathway. MSCs express a wide variety of G_s-coupled receptors for histamine, adenosine, dopamine and 5-HT (Fig. 1,A). Among investigated cAMP activating hormones only 5-HT was able to increase the portion of MSCs responding to noradrenaline by activation cytoplasmic Ca^{2+} influx (Fig. 1,B-H). 5-HT caused the elevation of α1A-adrenoceptors in MSCs (Fig. 1,J). Furthermore, α1A-adrenoceptors antagonist naftopidil abolished the 5-HT effect (Fig. 1,I). At the same time, neither 5-HT or noradrenaline affected the proportion of cells responding to 5-HT by the activation of Ca^{2+} influx (Fig. 1,K). These data indicate that 5-HT exerted a permissive effect on the MSCs sensitivity to noradrenaline via specific up-regulation of α1A-adrenoceptors.

As α1A-adrenoceptors are the key regulators of contraction of small vessels in adipose tissue, we examined whether 5-HT-dependent permissive action on α1A-adrenoceptors stimulates MSCs contraction. For this purpose, we used collagen disk retraction assay (Fig. 2). MSCs were polymerized into a 3D-collagen matrix and stimulated with 5 μM 5-HT followed by the second 1 μM noradrenaline addition 6 h later (Fig. 2, A). Collagen disc area was measured before stimulation with noradrenaline as well as 2 and 24 h after noradrenaline treatment (Fig. 2,B-E). Neither isolated noradrenaline or 5-HT treatment affected the collagen disk area. At the same time 5-HT permitted collagen disks shrinkage upon noradrenaline treatment (Fig. 2,E). 5-HT effect on noradrenaline-induced MSCs contractility is consistent with observed increase of Ca^{2+} influx. This effect was similar to noradrenaline-

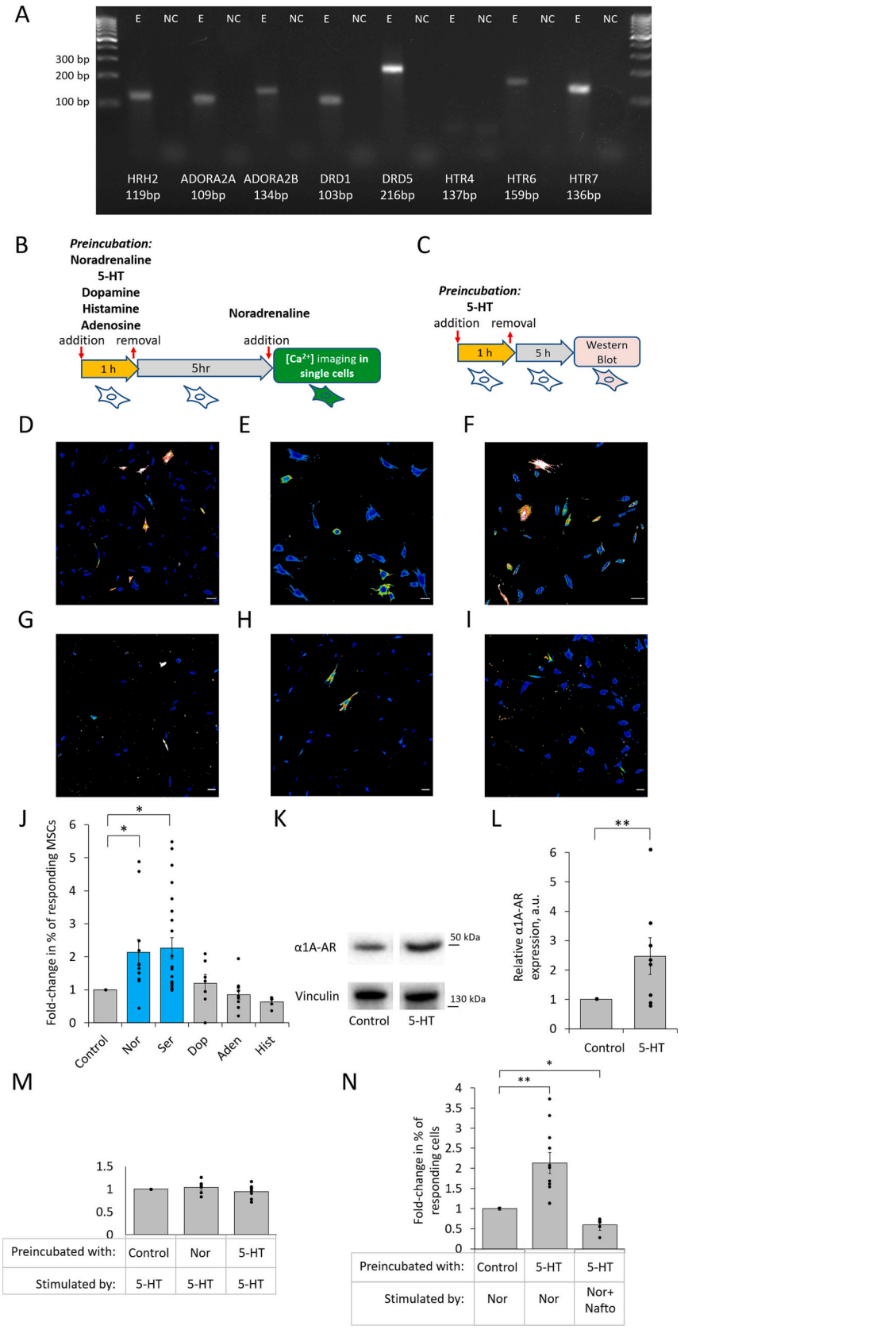

(caption on next page)

Fig. 1. 5-HT exerts a permissive effect on the noradrenaline-dependent calcium signaling in MSCs. (A) - PCR analysis of expression of cAMP-dependent isoforms of receptors to histamine (HRH2), adenosine (ADORA2A and ADORA2B), dopamine (DRD1 and DRD5), and 5-HT (HTR4, HTR6, and HTR7). E - experiment, NC - negative control. (B) – Pipeline of the experiment with measurement of calcium signaling. Cells were preincubated with cAMP mobilizing hormone (noradrenaline, 5-HT, dopamine, histamine, or adenosine) or vehicle (Control) for 1 h, and 5 h later subjected to noradrenaline treatment together with calcium imaging. (C) – Pipeline of the experiment with Western Blotting. Cells were preincubated with 5-HT or vehicle (Control) for 1 h, and 5 h later were lysed for Western Blot analysis. (D—I) – Representative images of responded MSCs in vehicle-treated cells (D) or after cAMP mobilizing hormones: (E) – noradrenaline (1 μM), (F) – 5-HT, (G) – dopamine (10 μM), (H) – adenosine (10 μM), (I) – histamine (1 μM). Scale bar 100 μm. (J) – Fold change in share of MSCs responded to noradrenaline 6 h after treatment with cAMP mobilizing hormone: Nor - noradrenaline (1 μM), 5-HT (10 μM), Dop - dopamine (10 μM), Aden - adenosine (10 μM), Hist - histamine (1 μM). Mean ± SEM, $n = 6$–10, * $p < 0.05$ (Mann-Whitney U Test). (K-L) Western blot analysis of α1A-adrenergic receptors after 5-HT treatment, (K) - representative images and (L) - quantification of bands intensity, $n = 8$, ** $p < 0.01$ (Mann-Whitney U Test). (M) - Fold change in share of MSCs responded to 5-HT (10 μM) 6 h after treatment with noradrenaline or 5-HT. Mean ± SEM, n = 6–7. (N) - Fold change in share of MSCs responded to noradrenaline (1 μM) or noradrenaline in the presence of α1-antagonist naftopidil (10 μM) 6 h after treatment with 5-HT. Mean ± SEM, $n = 6$.

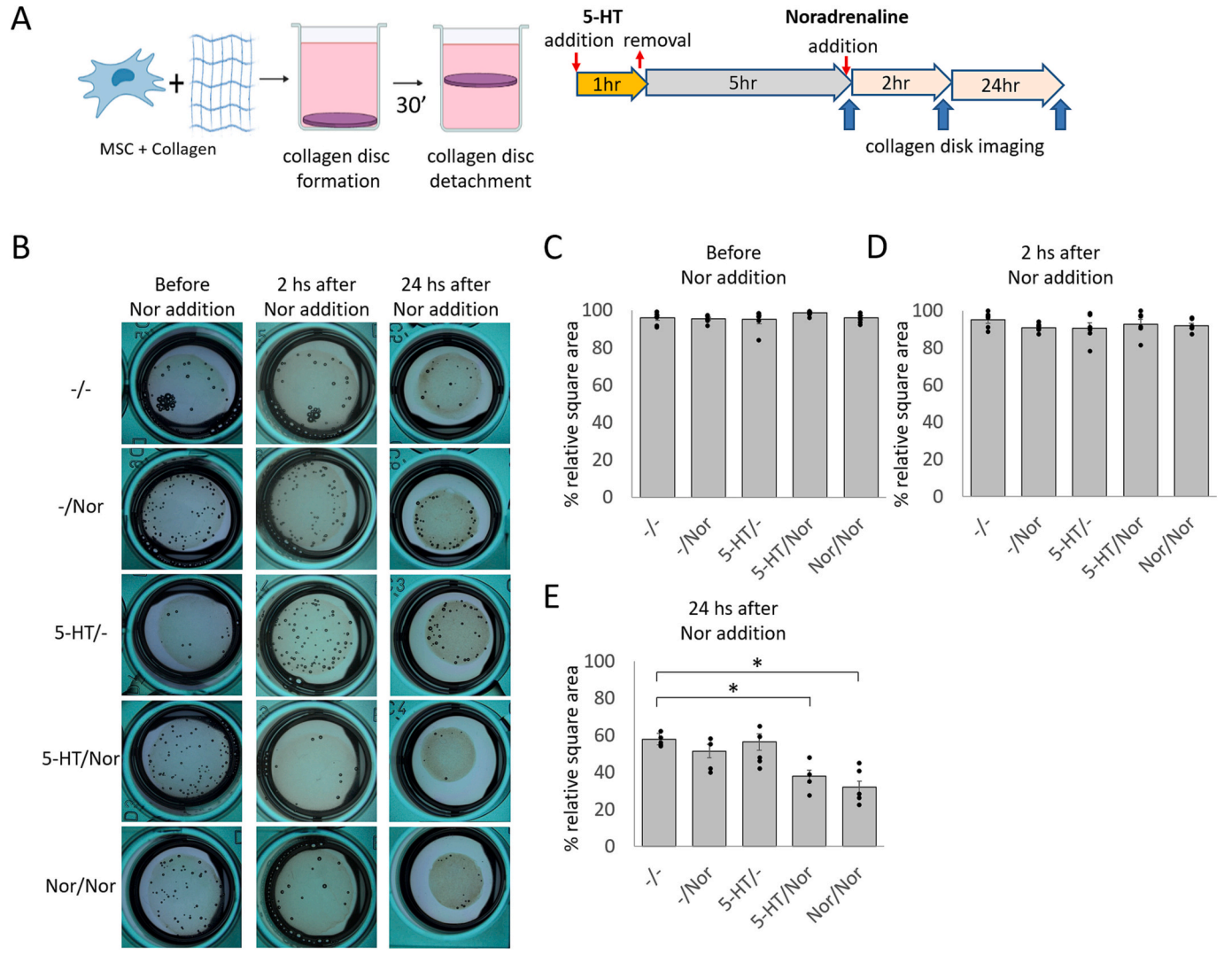

Fig. 2. 5-HT induces collagen disk shrinkage upon noradrenaline treatment. (A) Scheme of MSCs-containing collagen discs contraction assay. (B) Representative images of collagen disks with MSCs just before, 2 h or 24 h after noradrenaline addition. Vehicle treated MSCs (−/−), MSCs treated with noradrenaline alone (−/Nor); MSCs treated with 5-HT alone (5-HT/−); MSCs treated by noradrenaline 6 h after 5-HT or noradrenaline treatment (5-HT/Nor and Nor/Nor, respectively). (C-E), relative square area of collagen disks containing MSCs before (C), 2 h (D) and 24 h (E) after noradrenaline treatment. $n = 3$–6, * $p < 0.05$ calculated with Kruskal-Wallis One Way ANOVA on Ranks.

dependent potentiation of MSCs contractility via α1A-adrenergic receptors reported earlier [4].

3.2. 5-HT increases α1A-adrenoceptor signaling in adipose MSCs via HT receptor type 6

To identify specific isoforms of 5-HT receptors, which mediate the permissive action of 5-HT on the adrenergic sensitivity of MSCs, we used inhibitory analysis, using antagonists of cAMP-associated 5-HT receptors (HTR6 and HTR7), expressed by cultured MSCs. Pre-treatment of cells with HTR6 isoform-specific antagonist R1485 (1 μM) [17,18], completely prevented the 5-HT-mediated increase in noradrenaline-induced calcium signaling. At the same time, HTR7 inhibition with 10 μM SB258719 did not affect noradrenaline-induced calcium signaling

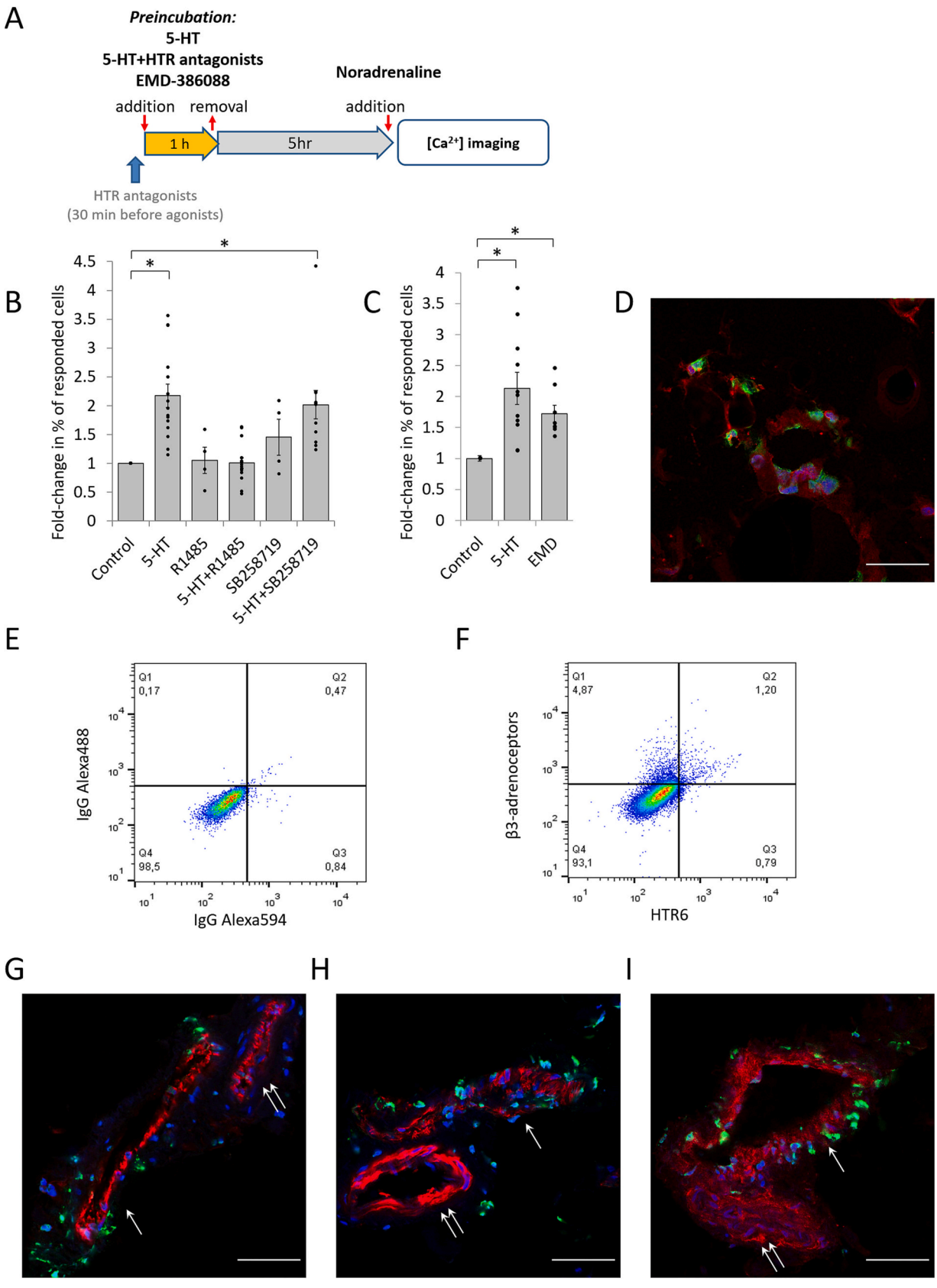

(caption on next page)

Fig. 3. HTR6 isoform mediates 5-HT effects in MSCs. (A) – Pipeline of the experiment. Cells were preincubated with 5-HT, 5-HT in the presence of HTR antagonists, HTR6 agonist EMD-386088, or vehicle (Control) for 1 h, and 5 h later subjected to noradrenaline treatment together with calcium imaging. (B) - Fold-change in the percentage of MSCs responded to noradrenaline after preincubation with 10 μM of 5-HT and 5-HT in the presence of HTR6 antagonist R1485 (1 μM), or HTR7 antagonist SB258719 (10 μM). $n = 4–15$, * $p < 0.05$ calculated with Kruskal–Wallis and one way ANOVA on ranks. (C) - Fold-change in the percentage of MSCs responded to noradrenaline after preincubation with 10 μM of 5-HT and 10 nM of potent HTR6 agonist EMD-386088. $n = 7$, * $p < 0.05$ calculated with Kruskal–Wallis and one way ANOVA on ranks. (D) - Confocal images of frozen sections of human subcutaneous adipose tissue. HTR6 (green) demonstrated the same distribution as β3-adrenoceptors (red) in perivascular regions of adipose tissue. Scale bar 50 μm. (*E*-F) – Flow cytometry analysis of HTR6 and β3-adrenoceptors expression in MSCs population (F) and appropriate IgG controls (E). (G-I) - Confocal images of frozen sections of human subcutaneous adipose tissue. (G) - HTR6 (green) localized near blood vessels out of CD31-expressing endothelium (CD31 - red staining). (H) - HTR6 (green) co-localized with αSMA expressing smooth muscle cells (red). (I) - HTR6 (green) co-localized with PDGFRβ expressing pericytes/MSCs. Single arrows mark the vessels expressing HTR6; double-arrows mark the vessels showing reduced expression of HTR6. Scale bar 50 μm.

(Fig. 3,A). According to the results of flow cytometry analysis, near 1–2 % of MSCs expressed HTR6, and all these cells also co-expressed β3-adrenoceptors (Fig. 3,B-C).

Since HTR6 was not previously associated with peripheral 5-HT effects, we have examined its spatial distribution in the adipose tissue. HTR6 receptor was localized within adipose tissue stoma. Predominantly HTR6-positive cells were associated with blood vessels and co-expressed markers of smooth muscle cells (αSMA) and pericytes/MSCs PDGFRβ but not the endothelium-specific CD31 (Fig. 3,C-E). Specifically, HTR6^{+} cells localized in small blood vessels and adventitial (the outmost) layer of larger vessel. Interestingly, that blood vessels in adipose tissue differed regarding the expression of HTR6. A number of vessels did not express HTR6 (vessels marked by the double-arrow in Fig. 3,F-H), while others expressed a large amount of receptor (vessels marked by the single-arrow in Fig. 3,F-H). HTR6 receptors were localized primarily in the same cells as β3-adrenoceptors within small vessels of adipose tissue (Fig. 3,C). The share of HTR6-positive cells in cultured MSCs isolated from adipose tissue was about 5 %. Consistently with in vivo data, the most of isolated HTR6-positive cells also expressed β3-adrenoceptors (Fig. 3,E).

To further confirm the impact of HTR6 receptor on the permissive action of 5-HT on adrenergic signaling we down-regulated this receptor using CRISPR-interference (CRISPRi system). Since MSCs, being stem cells, are effectively protected from genetic interventions, we used an hTert-immortalized line of adipose-derived MSCs (ASC52-telo). We reached a 40 % decrease in the HTR6 expression (Fig. 4,A-B), which fully prevented the 5-HT-mediated increase in noradrenaline-induced calcium signaling (Fig. 4,C-D). Suppression of the HTR6 level also canceled 5-HT permission for collagen disks shrinkage upon noradrenaline treatment (Fig. 4,*E*-G). These data suggest that HTR6 receptor isoform is responsible for 5-HT effect on adrenoceptors signaling/sensitivity in MSCs of adipose tissue and their contractility.

3.3. Permissive action of 5-HT on adrenergic signaling is associated with development of arterial hypertension

Since MSCs control noradrenaline-induced vascular contraction and thus could contribute to the development of obesity-associated hypertension we evaluated whether MSCs ability for 5-HT-induced increase in noradrenaline sensitivity and the cell's contractility are associated with obesity-linked hypertension. We compared cells isolated from subcutaneous adipose tissue of hypertensive and normotensive patients with obesity (Supplemental Table 1). 5-HT increased the portion of cells responding to noradrenaline by activation Ca^{2+} influx in MSCs isolated from obese hypertensive donors (Fig. 5,A). In contrast, 5-HT was not able to elevate MSCs sensitivity to noradrenaline in cells isolated from obese normotensive donors. The level of 5-HT-mediated increase in the noradrenaline responsiveness was well correlated with mean blood pressure and systolic blood pressure of obese patients, but not diastolic blood pressure (Fig. 5,B-D). These data well correlate with the fact that not all obese patients are hypertensive, whereas increased 5-HT concentration accompanies obesity in most cases [19] (Table 1).

4. Discussion

This study for the first time demonstrates that peripheral 5-HT exerts a permissive action on noradrenaline-induced contractility of MSCs associated with blood vessels of adipose tissue. 5-HT was initially discovered as a serum tone-regulating vasoconstrictive agent [20]. HTR2A was described as a major contractile-associated receptor isoform [21]. However pharmacological and genetic studies failed to fully confirm 5-HT effects on the vascular contractility [22]. Our data suggest a previously unrecognized mechanism of 5-HT action on vascular contraction. We showed that this effect of 5-HT was mediated by the HTR6, whose functions outside of the central nervous system were not previously defined [23,24].

Apparently, HTR6 was predominately associated with small blood vessels, and its presence in the outmost layer of larger blood vessels could also be related to small vessels, which provide a blood supply to the wall of larger ones (so called *vasa vasorum*). Microvasculature significantly contributes to the regulation of blood pressure (Katunaric B, et al. 2022). Therefore, the spatial distribution of HTR6 in small blood vessels fits in well with our data that 5-HT enhances noradrenaline-induced contractility of MSCs and that the magnitude of such elevation correlates with increased blood pressure of obese patients.

Our data also suggest a cooperative action of 5-HT and noradrenaline on MSCs contractility. Cooperative action of 5-HT and noradrenaline on vascular contractility was previously shown in a number of works. Some of the contractile effects of 5-HT were associated with activation of α1-adrenoceptors in isolated blood vessels [25]. In another work, addition of 5-HT to the isolated central artery of the rabbit ear leads to immediate (60 s after 5-HT addition) increase in the contractile response to noradrenaline. And, in turn, perfusion of the artery with noradrenaline increased 5-HT-dependent contractile response [26]. Another example of immediate potentiation of adrenergic-dependent blood vessel contraction by 5-HT was shown by Conti and co-authors [27]. These effects are dependent only on calcium mobilizing α1-adrenoceptors and HTR2 serotonergic receptors (reviewed in [28]). 5-HT-dependent potentiation of α1-adrenoceptors develops in 1 min and disappears 2 min after 5-HT washout [26]. Despite the precise molecular mechanisms of cooperative interactions of 5-HT and noradrenaline were not shown, one may suppose that they involve an increase in intracellular calcium level caused by the previous hormone, or the potentiation of calcium channels.

Another previously described mechanism of synergistic action of 5-HT and noradrenaline on vascular contraction involves the interaction of cAMP-dependent and calcium-dependent signaling. Here 5-HT via Gi-coupled HTR1 down-regulated intracellular cAMP level and thus led to potentiation of calcium-dependent effects of noradrenaline, angiotensin II, and endothelin [28,29].

In contrast to previously described mechanisms, 5-HT effect on adipose MSCs observed in this study was not immediate and required at least 6 h. We also did not observe an inverse noradrenaline-dependent potentiation of 5-HT signaling. Importantly, it was mediated by cAMP-activating HTR6, Gs-associated GPCR that was previously thought to be expressed exclusively in the central nervous system [30]. HTR6 is primarily expressed in the regions of the brain involved in cognitive

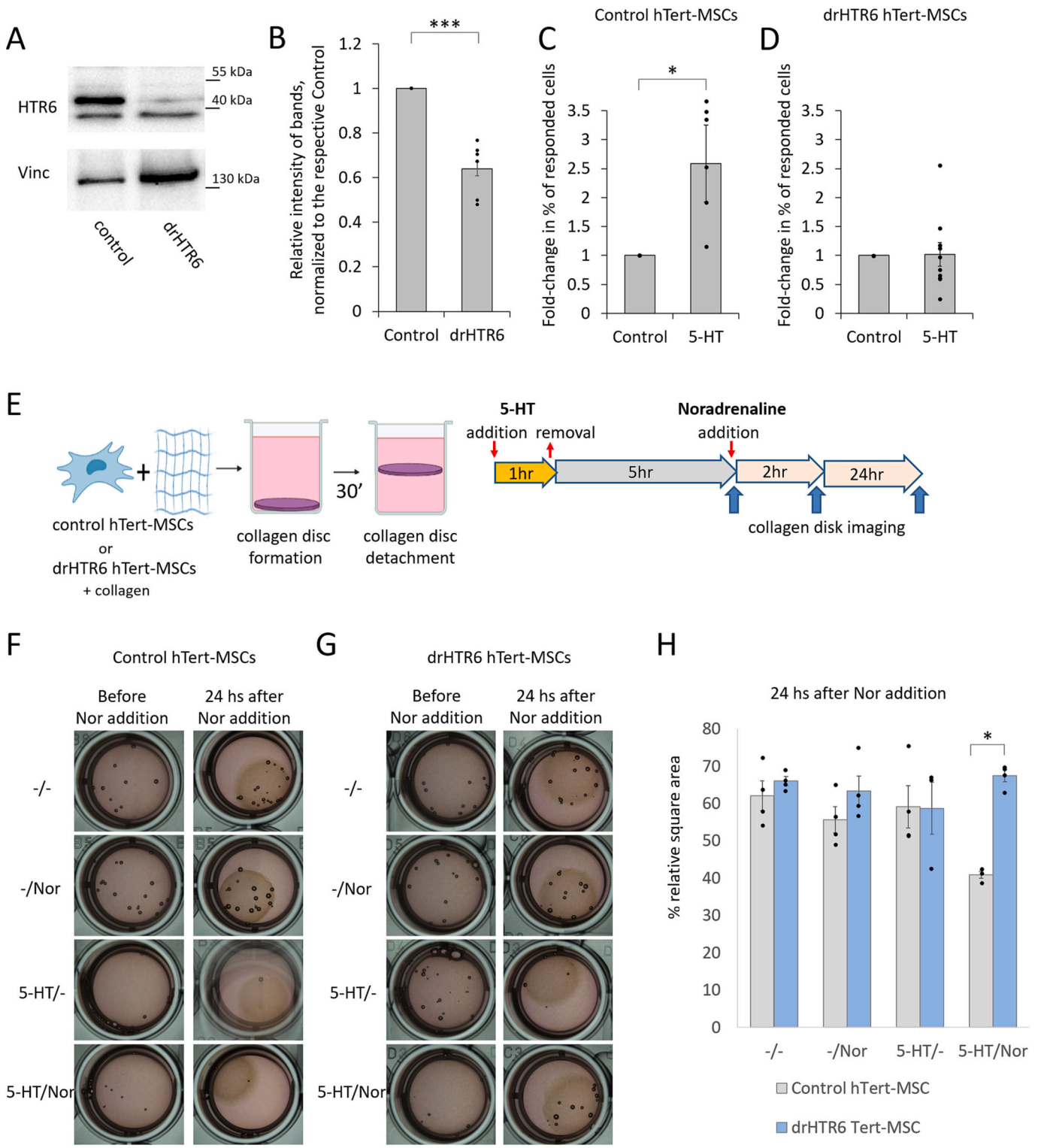

Fig. 4. The HTR6 down-regulation canceled the effect of 5-HT on MSC contractility. (A-B) HTR6 down-regulation using CRISPR-Cas9 assay. Western blot analysis of HTR6 receptor expression, (A) - representative images and (B) - quantification of bands intensity, $n = 6$, *** $p < 0.001$ (Student's *t*-test). (C-D) Fold-change in the percent of MSCs responded to noradrenaline after 5-HT treatment (5-HT) in control ASC52telo cells (Control ASC52-telo) or cells after HTR6 down-regulation (drHTR6 ASC52-telo). n = 6–7, * $p < 0.05$ (Student's t-test). (E-H) Collagen discs assay to measure contractile properties of MSCs. (E) – Pipeline of collagen discs assay. Cells were *co*-polymerized with type 1 collagen, MSCs-collagen discs were detached, and after that cells were preincubated with 5-HT or vehicle (−) for 1 h, and 5 h later cells were treated with noradrenaline (Nor) or vehicle (−). Size of MSCs-collagen discs was measured 2 h and 24 h later. (F-G) Collagen disks with (F) control ASC52telo cells (Control ASC52-telo) or (G) cells after HTR6 down-regulation (drHTR6 ASC52-telo) just before noradrenaline addition and 24 h after noradrenaline addition. Vehicle treated cells (−/−), cells treated with noradrenaline alone (−/Nor); cells treated with 5-HT alone (5-HT/−) without followed noradrenaline treatment; cells treated by noradrenaline 6 h after 5-HT treatment (5-HT/Nor). (H) – Relative square area of collagen disks containing MSCs 24 h after noradrenaline treatment. $n = 3$, * $p < 0.05$ (Kruskal-Wallis One Way ANOVA on Ranks).

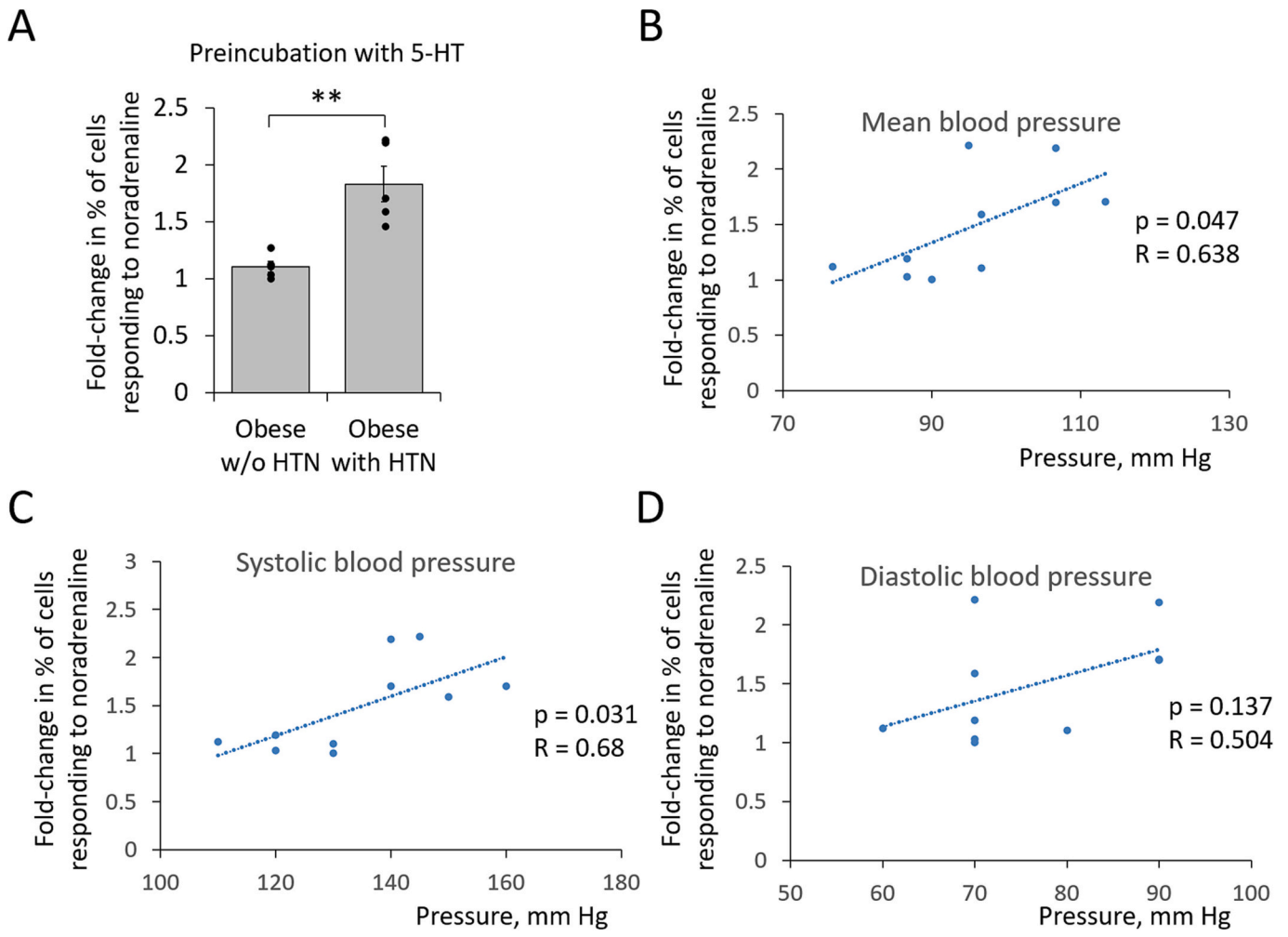

Fig. 5. Permissive action of 5-HT on adrenergic signaling is correlated with development of arterial hypertension in the patients with obesity. (A) Fold-change in share of MSCs from obese donors with or without hypertension responded to noradrenaline 6 h after 5-HT, mean ± SEM, $n = 5–7$, ** $p < 0.01$ (Mann-Whitney U Test). (B-D) Correlation between mean (B), systolic (C), and diastolic (D) blood pressure and the magnitude of MSC's response to noradrenaline after 5-HT. HTN - hypertension.

Table 1
5-HT dependent permissive effect in normotensive and hypertensive patients.

Patient code	Ethnicity	Age (years)	BMI (kg/m^2)	Gender	SBP/DBP[a]	Arterial hypertension	5-HT dependent permissive effect
1	Caucasian	50	32.96	Male	130/80	–	1.10
2	Caucasian	45	34.26	Male	120/70	–	1.27
3	Caucasian	38	30.19	Male	130/70	–	1.00
4	Caucasian	39	33.00	Male	110/60	–	1.12
5	Caucasian	28	33.00	Male	125/70	–	1.03
6	Caucasian	38	30.00	Male	145/70	+	2.22
7	Caucasian	56	31.56	Male	150/70	+	1.46
8	Caucasian	62	32.95	Male	140/90	+	1.59
9	Caucasian	38	38.51	Male	160/90	+	1.70
10	Caucasian	47	35.32	Female	140/90	+	2.19

[a] SBP/DBP – systolic blood pressure/diastolic blood pressure.

functions, thus it is intensively studied as a target for the treatment of cognitive deficits of various neuropsychiatric diseases such as Alzheimer's disease and schizophrenia [30,31]. Here we have got the first evidence of the functioning of HTR6 in the periphery and found that MSCs are targets for peripheral 5-HT effects via HTR6.

Important finding of this study is that among heterogeneous multiplicity of adipose MSCs, HTR6-positive cells represent only about 1–2 %. According to our results in situ and in vitro, the majority of HTR6-positive MSCs co-express β3-adrenoceptor, which previously was reported as a trigger involved in the development of obesity-associated hypertension [4]. Since these receptors enhance contractile properties of MSCs, we may speculate that identified ADRB3$^+$/HTR6$^+$ cells in adipose tissue are involved in the hormonal regulation of vascular contraction. This particular MSCs subpopulation could therefore be implicated in the development of obesity-associated hypertension. Furthermore, the HTR6-dependent increase in the sensitivity of MSCs to noradrenaline and the associated increase in their contractility make HTR6 a novel pharmacological target for the prevention of such pathological

conditions.

Supplementary data to this article can be found online at https://doi.org/10.1016/j.bbamcr.2023.119651.

Funding

This work was supported by Russian Science Foundation grant #19-75-30007 (https://rscf.ru/project/19-75-30007/, flow cytometry, CRISPRi, Collagen gel contraction assay, Immunofluorescent analysis) and Russian Science Foundation grant #21-15-00311 (https://rscf.ru/project/21-15-00311/, calcium imaging, inhibitory analysis).

CRediT authorship contribution statement

Vadim I. Chechekhin: Writing – review & editing, Writing – original draft, Visualization, Validation, Software, Methodology, Investigation, Formal analysis, Data curation, Conceptualization. **Anastasia M. Ivanova:** Investigation, Formal analysis. **Konstantin Y. Kulebyakin:** Writing – review & editing, Writing – original draft, Methodology, Formal analysis, Data curation. **Yulia G. Antropova:** Investigation, Data curation. **Maxim N. Karagyaur:** Methodology, Investigation. **Maria N. Skryabina:** Methodology, Investigation. **Elizaveta S. Chechekhina:** Investigation. **Natalia A. Basalova:** Methodology, Investigation. **Olga A. Grigorieva:** Methodology, Investigation. **Veronika Yu Sysoeva:** Methodology, Investigation. **Natalia I. Kalinina:** Writing – review & editing, Writing – original draft, Validation, Methodology, Investigation, Data curation, Conceptualization. **Vsevolod A. Tkachuk:** Supervision, Resources, Funding acquisition, Conceptualization. **Pyotr A. Tyurin-Kuzmin:** Writing – review & editing, Writing – original draft, Visualization, Validation, Supervision, Resources, Project administration, Methodology, Investigation, Funding acquisition, Formal analysis, Data curation, Conceptualization.

Declaration of competing interest

The authors declare that they have no known competing financial interests or personal relationships that could have appeared to influence the work reported in this paper.

Data availability

No data was used for the research described in the article.

Acknowledgments

We thank Dr. Alexander Velikanov for assistance with flow cytometry experiments. Experiments were conducted using equipment purchased as part of the MSU Development Program.

References

[1] P. Bourin, B.A. Bunnell, L. Casteilla, M. Dominici, A.J. Katz, K.L. March, H. Redl, J. P. Rubin, K. Yoshimura, J.M. Gimble, Stromal cells from the adipose tissue-derived stromal vascular fraction and culture expanded adipose tissue-derived stromal/stem cells: a joint statement of the International Federation for Adipose Therapeutics and Science (IFATS) and the International Society for Cellular Therapy (ISCT), Cytotherapy 15 (2013) 641–648, https://doi.org/10.1016/j.jcyt.2013.02.006S1465-3249(13)00387-3 [pii].

[2] V.I. Chechekhin, K. Kulebyakin, R.I. Kokaev, P.A. Tyurin-Kuzmin, GPCRs in regulation of functional activity of multipotent mesenchymal stromal cells, Frontiers in Cell and Developmental Biology (2022) 1512.

[3] A.I. Caplan, New MSC: MSCs as pericytes are sentinels and gatekeepers, J. Orth. Res. 35 (2017) 1151–1159.

[4] V. Chechekhin, A. Ivanova, K. Kulebyakin, V. Sysoeva, D. Naida, M. Arbatsky, N. Basalova, M. Karagyaur, M. Skryabina, A. Efimenko, O. Grigorieva, N. Kalinina, V. Tkachuk, P. Tyurin-Kuzmin, Alpha1A-and Beta3-adrenoceptors interplay in adipose multipotent mesenchymal stromal cells: a novel mechanism of obesity-driven hypertension, Cells 12 (2023) 585.

[5] P.A. Tyurin-Kuzmin, D.T. Dyikanov, J.I. Fadeeva, V.Y. Sysoeva, N.I. Kalinina, Flow cytometry analysis of adrenoceptors expression in human adipose-derived mesenchymal stem/stromal cells, Sci Data 5 (2018), 180196, https://doi.org/10.1038/sdata.2018.196sdata2018196 [pii].

[6] P.A. Tyurin-Kuzmin, J.I. Fadeeva, M.A. Kanareikina, N.I. Kalinina, V.Y. Sysoeva, D. T. Dyikanov, D.V. Stambolsky, V.A. Tkachuk, Activation of beta-adrenergic receptors is required for elevated alpha1A-adrenoreceptors expression and signaling in mesenchymal stromal cells, Sci. Rep. 6 (2016) 32835, https://doi.org/10.1038/srep32835srep32835 [pii].

[7] P.A. Tyurin-Kuzmin, M.N. Karagyaur, K.Y. Kulebyakin, D.T. Dyikanov, V. I. Chechekhin, A.M. Ivanova, M.N. Skryabina, M.S. Arbatskiy, V.Y. Sysoeva, N. I. Kalinina, Functional heterogeneity of protein kinase a activation in multipotent stromal cells, Int. J. Mol. Sci. 21 (2020) 4442.

[8] B.I. Gustafsson, L. Thommesen, A.K. Stunes, K. Tommeras, I. Westbroek, H. L. Waldum, K. Slordahl, M.V. Tamburstuen, J.E. Reseland, U. Syversen, Serotonin and fluoxetine modulate bone cell function in vitro, J. Cell. Biochem. 98 (2006) 139–151, https://doi.org/10.1002/jcb.20734.

[9] R.R. Pochampally, J. Ylostalo, P. Penfornis, R.R. Matz, J.R. Smith, D.J. Prockop, Histamine receptor H1 and dermatopontin: new downstream targets of the vitamin D receptor, J. Bone Miner. Res. 22 (2007) 1338–1349.

[10] P.A. Zuk, M. Zhu, H. Mizuno, J. Huang, J.W. Futrell, A.J. Katz, P. Benhaim, H. P. Lorenz, M.H. Hedrick, Multilineage cells from human adipose tissue: implications for cell-based therapies, Tissue Eng. 7 (2001) 211–228, https://doi.org/10.1089/107632701300062859.

[11] K. Kulebyakin, P. Tyurin-Kuzmin, L. Sozaeva, N. Voloshin, M. Nikolaev, V. Chechekhin, M. Vigovskiy, V. Sysoeva, E. Korchagina, D. Naida, M. Vorontsova, Dynamic balance between PTH1R-dependent signal cascades determines its pro-or anti-osteogenic effects on MSC, Cells 11 (2022) 3519.

[12] K. Kulebyakin, P. Tyurin-Kuzmin, A. Efimenko, N. Voloshin, A. Kartoshkin, M. Karagyaur, O. Grigorieva, E. Novoseletskaya, V. Sysoeva, P. Makarevich, Decreased insulin sensitivity in telomerase-immortalized mesenchymal stem cells affects efficacy and outcome of adipogenic differentiation in vitro, Frontiers in Cell and Developmental Biology 9 (2021), 662078.

[13] P. Ngo, P. Ramalingam, J.A. Phillips, G.T. Furuta, Collagen gel contraction assay, Cell-Cell Interactions (2006) 103–109.

[14] M.H. Larson, L.A. Gilbert, X. Wang, W.A. Lim, J.S. Weissman, L.S. Qi, CRISPR interference (CRISPRi) for sequence-specific control of gene expression, Nat. Protoc. 8 (2013) 2180–2196.

[15] M. Karagyaur, Y.P. Rubtsov, P. Vasiliev, V. Tkachuk, Practical recommendations for improving efficiency and accuracy of the CRISPR/Cas9 genome editing system, Biochem. Mosc. 83 (2018) 629–642.

[16] P.A. Longo, J.M. Kavran, M.-S. Kim, D.J. Leahy, Transient mammalian cell transfection with polyethylenimine (PEI), Methods Enzymol., Elsevier (2013) 227–240.

[17] F. Borsini, Pharmacology of 5-HT6 Receptors, Academic Press, 2011.

[18] S.-H. Zhao, J. Berger, R.D. Clark, S.G. Sethofer, N.E. Krauss, J.M. Brothers, R. S. Martin, D.L. Misner, D. Schwab, L. Alexandrova, 3, 4-Dihydro-2H-benzo [1, 4] oxazine derivatives as 5-HT6 receptor antagonists, Bioorg. Med. Chem. Lett. 17 (2007) 3504–3507.

[19] R.L. Young, A.L. Lumsden, A.M. Martin, G. Schober, N. Pezos, S.S. Thazhath, N. J. Isaacs, N. Cvijanovic, E.W. Sun, T. Wu, Augmented capacity for peripheral serotonin release in human obesity, Int. J. Obesity 42 (2018) 1880–1889.

[20] M.M. Rapport, A.A. Green, I.H. Page, Crystalline serotonin, Science 108 (1948) 329–330.

[21] S.W. Watts, Serotonin-induced contraction in mesenteric resistance arteries: signaling and changes in deoxycorticosterone acetate–salt hypertension, Hypertension 39 (2002) 825–829.

[22] S.W. Watts, S.F. Morrison, R.P. Davis, S.M. Barman, Serotonin and blood pressure regulation, Pharmacol. Rev. 64 (2012) 359–388.

[23] D.E. Nichols, C.D. Nichols, Serotonin receptors, Chem. Rev. 108 (2008) 1614–1641.

[24] J.D. McCorvy, B.L. Roth, Structure and function of serotonin G protein-coupled receptors, Pharmacol. Ther. 150 (2015) 129–142.

[25] R. Purdy, D. Murray, G. Stupecky, Receptors for 5-hydroxytryptamine in rabbit blood vessels: activation of alpha adrenoceptors in rabbit thoracic aorta, J. Pharmacol. Exp. Ther. 240 (1987) 535–541.

[26] I. De La Lande, V.A. Cannell, J. Waterson, The interaction of serotonin and noradrenaline on the perfused artery, Br. J. Pharmacol. Chemother. 28 (1966) 255.

[27] A. Conti, A. Monopoli, A. Forlani, E. Ongini, C. Antona, P. Biglioli, Role of 5-HT2 receptors in serotonin-induced contraction in the human mammary artery, Eur. J. Pharmacol. 176 (1990) 207–212.

[28] O. Yildiz, J. Smith, R. Purdy, Serotonin and vasoconstrictor synergism, Life Sci. 62 (1998) 1723–1732.

[29] H. Movahedi, H.T. Le, H.M. Spanggord, R.E. Purdy, Effect of alpha adrenergic agonist on the rabbit ear artery contraction to serotonin: enhanced response mediated by serotonergic1-like receptors, J. Pharmacol. Exp. Ther. 272 (1995) 364–370.

[30] S. Chaumont-Dubel, V. Dupuy, J. Bockaert, C. Becamel, P. Marin, The 5-HT6 receptor interactome: new insight in receptor signaling and its impact on brain physiology and pathologies, Neuropharmacology 172 (2020), 107839.

[31] D. Marazziti, S. Baroni, F. Borsini, M. Picchetti, E. Vatteroni, V. Falaschi, M. Catena-Dell'Osso, Serotonin receptors of type 6 (5-HT6): from neuroscience to clinical pharmacology, Curr. Med. Chem. 20 (2013) 371–377.